

# Chapter 12

## Chemistry in the Atmospheric Boundary Layer

J. Vilà-Guerau de Arellano<sup>1</sup> and J. Lelieveld<sup>2</sup>

<sup>1</sup>*Departament Física Aplicada, Universitat Politècnica de Catalunya,  
Barcelona, Spain.*

<sup>2</sup>*Institute for Marine and Atmospheric Research at Utrecht University,  
Utrecht, The Netherlands.*

---

### Abstract

The basic concepts of chemistry in the atmospheric boundary layer are described. The governing equations and dimensionless parameters are derived for this turbulent reacting flow. Prototypes of the atmospheric boundary layer with chemically reactive species are presented to illustrate the current knowledge of the subject. Some examples of parameterizations to account for the effect of the physical processes on atmospheric chemistry are given.

---

### 1 Introduction

Atmospheric chemistry addresses the physical and chemical interactions between relatively short-lived species. The influence of physical processes on chemical transformations in the lower troposphere is the key issue in this chapter. The transport and turbulent mixing of chemical species as well as ultraviolet radiation constitute the driving forces of tropospheric chemistry. Although clouds occupy only 10% of the volume in the lower troposphere, their presence enables important aqueous-phase chemical pathways and they modify photochemical reaction rates because the radiation field is strongly perturbed.

Chemical species are emitted by natural or antropogenic sources into the Atmospheric Boundary Layer (ABL). Important species such as ozone are

entrained from the free troposphere into the ABL. These primary species undergo chemical transformations and, as a consequence, secondary compounds are produced. Finally, primary and secondary compounds are transported to the free troposphere or are deposited on the Earth's surface. Hence, the ABL can be regarded as a photochemical reaction vessel that is influenced by mass exchanges at the boundaries and is regulated by atmospheric physical processes.

The purpose of this chapter is threefold: we first introduce the fundamental concepts that are needed to understand the distribution and the evolution of chemical species in the ABL. The main governing equations and dimensionless parameters are derived and a classification is given of turbulent reacting flows in the ABL (section 2). Second, we show the relevant influences of the ABL processes on chemical reactions; detailed examples of archetypical ABL's are given in which species are chemically transformed (section 3). Third, we introduce various parameterizations which take into account the effect that the ABL characteristics and processes have on chemical reactions (section 4). These descriptions can be used in large-scale atmospheric chemistry models.

This chapter is intended to be supplementary to some of the main text books and review articles that deal with atmospheric chemistry and turbulent reacting flows (Libby and Williams, 1980; Finlayson-Pitts and Pitts, 1986; Seinfeld, 1986; Warneck, 1987; Pope, 1990; Bilger, 1992).

## 2 Governing equation for chemically reactive species

To determine the evolution of chemical species in the atmospheric boundary layer, one needs to solve not only the flow-governing equations, but also the conservation equation of chemical species. The concentration (mass per volume) of each constituent must satisfy the following equation (Lamb and Seinfeld, 1973)

$$\frac{\partial c_i}{\partial t} + \frac{\partial(u_\alpha c_i)}{\partial x_\alpha} = D_i \left( \frac{\partial^2 c_i}{\partial x_\alpha \partial x_\alpha} \right) + R_i(c_1, \dots, c_N, T, F) + S_i(x, t), \quad (1)$$

where  $c_i$  is the instantaneous concentration of species  $i$ ,  $t$  is time,  $u_\alpha$  is the  $\alpha$ -component of the wind velocity,  $x_\alpha$  is the  $\alpha$ -component of the space variable,  $D_i$  is the molecular diffusivity,  $R_i$  is the rate of chemical production or loss,  $N$  is the total number of chemical species,  $T$  is the temperature,  $F$  is the actinic flux (of photochemically active radiation) and  $S_i$  accounts for the sources and sinks. The Greek subscript  $\alpha$  in a term indicates summation over the three

components of the term. The chemical term in (1) can be written explicitly as

$$R_i = \sum_{j=1}^M \eta_{ij} k_j \prod_{l=1}^N c_l^{\beta_{lj}}, \quad (2)$$

where  $\eta_{ij}$  is the stoichiometric coefficient for species  $i$  in reaction  $j$ ,  $k_j$  is the reaction rate constant for reaction  $j$  and  $\beta_{lj}$  is the reaction order of species  $l$  in reaction  $j$ .  $M$  is the total number of reactions that species  $i$  undergoes. The dependence of the reaction term on the temperature and actinic flux is included in the reaction rate  $k_j$ .

By defining the following scales of the turbulent reacting flow: length (L), velocity (U), temperature (T) and concentration ( $C_{0i}$ ,  $i=1, \dots, N$ ); one can formulate equation (1) in a dimensionless form

$$\frac{\partial \tilde{c}_i}{\partial \tilde{t}} + \frac{\partial(\tilde{u}_\alpha \tilde{c}_i)}{\partial \tilde{x}_\alpha} = (Re Sc_i)^{-1} \left( \frac{\partial^2 \tilde{c}_i}{\partial \tilde{x}_\alpha \partial \tilde{x}_\alpha} \right) + \tilde{R}_i(\tilde{c}_1, \dots, \tilde{c}_N, \tilde{T}, \tilde{F}) + \tilde{S}_i(\tilde{x}, \tilde{t}), \quad (3)$$

where the symbol  $\sim$  refers to a dimensionless variable,  $Re$  is the Reynolds number and  $Sc_i$  is the Schmidt number (the ratio of the kinematic viscosity to the molecular diffusivity of species  $i$ ). The dimensionless reaction term  $\tilde{R}_i$  reads

$$\tilde{R}_i = \sum_{j=1}^M \eta_{ij} Da_j \prod_{l=1}^N \tilde{c}_l^{\beta_{lj}}. \quad (4)$$

In (4),  $Da_j$  is the Damköhler number of species  $i$  with respect to reaction  $j$  defined as

$$Da_j = \left( \frac{L}{U} \right) k_j \prod_{l=1}^N \left( \frac{C_{0l}^{\beta_{lj}}}{C_{0i}} \right). \quad (5)$$

This dimensionless number depends on the ratio of the flow time scale  $L/U$  to the chemical time scale, which varies according to the reaction order, and the ratio of the concentration scales. As this non-dimensional number shows, it is possible that reactions with large values of the chemical reaction rate are characterized by a relatively small  $Da_j$  due to their low concentrations in the ABL.

### 2.1 Analysis of scales in the ABL

The ABL is generally in a turbulent state with typical Reynolds numbers of  $10^7$  and Schmidt numbers around 1. Hence,  $(Re Sc_i)^{-1}$  is generally a small

number. Consequently, the molecular diffusivity term can be omitted from equation (3).

Based on the absolute value of the Damköhler number, the following classification for the turbulent reacting flows in the ABL can be established:

- **Slow chemistry** ( $Da_j \ll 1$ ). In equation (3) the chemical term is much smaller than the transport terms. Consequently, the chemical term can be neglected and chemical transformation of these species can be treated separately from the flow-governing equations. Compounds that react under this regime are referred to as long-lived species.
- **Moderate chemistry** ( $Da_j = O(1)$ ). There is a coupling between the flow and the chemistry. In the ABL, due to the relatively low concentrations (densities) of the reactive compounds, the chemistry does not modify the flow patterns. However, the flow *influences* the chemical transformations. All the terms in equation (3) should be treated explicitly and simultaneously.
- **Fast chemistry** ( $Da_j \gg 1$ ). The chemistry term can be dominant with respect to the other transport terms. Equation (3) reduces to  $\tilde{R}_i \simeq 0$ , the so-called pseudo-stationary state. The flow variables can be treated and solved separately from the chemical variables. Compounds that react under this regime are referred to as short-lived species.

Table 1. Typical time scales of transformations of chemical species and of some atmospheric phenomena. Here index  $b$  refers to the atmospheric boundary layer and  $t$  to the free troposphere.

Approximate time scale (s)	Chemical species	Atmospherica phenomena
$10^{-1} - 1$	$OH$	Turbulence
$10^2 - 10^3$	$NO, NO_2$	Thermal updrafts
$10^3 - 10^4$	$CH_2O, \text{isoprene}$	Convection, thunderstorms
$10^5 - 10^6$	$H_2O, SO_2^b, NO_x^b$	Synoptic weather fronts
$10^7$	$O_3^t, CO$	General circulation
$10^8 - 10^9$	$CH_4$	Climate changes

Table 1 shows the large span of time scales associated with atmospheric phenomena and the chemical transformation time scales of some important atmospheric compounds. From this table, it is clearly observed that a complete chemical scheme for the ABL can contain species that react in all three above-mentioned regimes.

## 2.2 First- and Second-Moment Reynolds Averaged Equations

It is not feasible to solve all the relevant spatial and time scales of the atmospheric flow. As a consequence, equation (3) must be solved in terms of the statistical moments of the concentration distribution. The wind and the concentration variables are decomposed into an average component ( $u_\alpha$  and  $c_i$ , i.e. first moments or mean) and a fluctuation or stochastic component ( $u'_\alpha$  and  $c'_i$ ), i.e. the Reynolds decomposition. Several kinds of averages, can be applied to the governing equations of the chemical species: the ensemble average, the time average, the one-dimensional average or the volume average (Garratt, 1992).

Applying the Reynolds decomposition to the variables  $u_\alpha$  and  $c_i$ , the Reynolds averaging properties, and making use of the continuity equation, one arrives at the following form for equation (3):

$$\frac{\partial \tilde{c}_i}{\partial \tilde{t}} + \tilde{u}_\alpha \frac{\partial \tilde{c}_i}{\partial \tilde{x}_\alpha} + \overline{\frac{\partial u'_\alpha c'_i}{\partial \tilde{x}_\alpha}} = \tilde{R}_i + \tilde{S}_i, \quad (6)$$

with the following chemical term  $\tilde{R}_i$

$$\tilde{R}_i = \sum_{j=1}^M \eta_{ij} Da_j \overline{\prod_{l=1}^N (\tilde{c}_l + c'_l)^{\beta_{lj}}}. \quad (7)$$

In the ABL, the main reactions of chemical species are of first- or second-order. Important third-order reactions can generally be reduced to quasi second-order chemical reactions. Therefore, one can assume that the order of reactions is equal to or smaller than 2, i.e. ( $\sum_{l=1}^N \beta_{lj} \leq 2$ ); and in that case the non-dimensional chemical term in the average concentration equation reads

$$\tilde{R}_i = \sum_{j=1}^M \eta_{ij} Da_j \left[ \prod_{l=1}^N \tilde{c}_l^{\beta_{lj}} + \overline{\prod_{l=1}^N c'_l{}^{\beta_{lj}}} \right]. \quad (8)$$

Equation (6) governs the average concentration and contains the new terms  $\overline{u'_\alpha c'_i}$  and  $\overline{\prod_{l=1}^N c'_l{}^{\beta_{lj}}}$ , i.e. second-order moments. The presence of these terms leads to the usual closure problem: there are more unknown terms than equations to solve them. In equation (6), the term  $\overline{u'_\alpha c'_i}$  is the concentration turbulent flux. The term describes important processes in the ABL such as exchange between the free troposphere and the ABL, turbulent transport, mixing in the ABL and deposition at the surface. The term  $\overline{\prod_{l=1}^N c'_l{}^{\beta_{lj}}}$  accounts for the variances and covariances. It describes how the rapid turbulent fluctuations influence the average concentration distribution and it quantifies the capacity

of turbulent reacting flows to mix chemical species. The Reynolds averaged governing equations for the second-order moments; with suitable parameterizations of the pressure gradient term, the dissipation term and the third-order terms, allow one to close the average concentration equation. The derivation of these second-order equations can be found elsewhere (Stull, 1988; Garratt, 1992).

In this chapter, we concentrate on the chemical terms in the second-order moment equations for chemically reactive species. They are derived in a dimensional form. Note that the terms are written in a general and compact form. In this way, and after algebraic manipulation, one can derive the chemical term for the first-, second- or higher-order reactions explicitly.

The chemical term in the governing equation for the concentration turbulent flux  $\overline{u'_\alpha \tilde{c}'_i}$  reads

$$R_{u'_\alpha \tilde{c}'_i} = \sum_{j=1}^M \eta_{ij} k_j \overline{u'_\alpha \prod_{l=1}^N (c_l + c'_l)^{\beta_{lj}}}, \quad (9)$$

The chemical term in the variance equation  $\overline{c_i'^2}$  can be written as

$$R_{c_i'^2} = 2 \sum_{j=1}^M \eta_{ij} k_j \overline{c'_i \prod_{l=1}^N (c_l + c'_l)^{\beta_{lj}}}, \quad (10)$$

and, finally, the chemical term in the governing equation for the covariance between two different species  $\overline{c'_i c'_k}$ ,  $i \neq k$  is

$$R_{c'_i c'_k} = \sum_{k=1}^N \sum_{j=1}^M \eta_{ij} k_j \overline{c'_k \prod_{l=1}^N (c_l + c'_l)^{\beta_{lj}}}. \quad (11)$$

It is important to notice that the non-dimensional form of the chemical terms (9), (10) and (11) introduces a Damköhler number which is now a function of the concentration flux scales instead of the concentration scales, i.e. the flux Damköhler number. The concentration flux scale is defined as the ratio of the flux of species  $i$  to a characteristic velocity scale. The derivation and analysis of these dimensionless equations can be found elsewhere (Vilà-Guerau de Arellano et al., 1995).

In order to solve the complete set of second-moments equations, one needs to add the equations for momentum and temperature to the second-moment concentration equations (see chapter 4).

### 2.3 Segregation of species

It is important to quantify the mixing state that is driven by the turbulence of the ABL and to determine how this state influences the chemical reactions. An adequate coefficient can be derived from (8), namely the **intensity or coefficient of segregation** (Danckwerts, 1953). Using once again the assumption  $\sum_{l=1}^N \beta_{lj} \leq 2$  and factorizing equation (8) one obtains

$$\tilde{R}_i = \sum_{j=1}^M \eta_{ij} Da_j \left[ \prod_{l=1}^N \tilde{c}_l^{\beta_{lj}} (1 + Is_j) \right], \quad (12)$$

where  $Is_j$  is the intensity of segregation for reaction  $j$  defined as follows

$$Is_j \equiv \frac{\overline{\prod_{l=1}^N \tilde{c}_l^{\beta_{lj}}}}{\prod_{l=1}^N \tilde{c}_l^{\beta_{lj}}}. \quad (13)$$

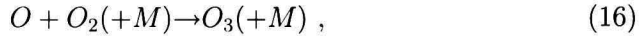
Notice that this term is the covariance of concentrations, which has been normalised by the product of the mean concentrations. The limiting values of  $Is$  depend on the Damköhler number and the transport direction of the species. The extreme minimum value is  $Is = -1$ . It corresponds to the situation in which species are transported in opposite directions (non-premixed reactants case) and the chemical reaction rate is infinitely fast, i.e.  $Da_j \rightarrow \infty$ . In that case, reaction takes place in an infinitely thin zone. The maximum limiting value,  $Is = \infty$ , is also given by a reaction characterized by a  $Da_j \rightarrow \infty$ . In that situation, species are transported in the same direction and have been previously homogeneously mixed, i.e. a case of premixed reactants.

## 3 Chemically reactive ABL

### 3.1 Surface layer

The first studies on the influence of turbulence on chemical reactions focused on the layer closest to the surface, the so-called surface layer (Lenschow, 1982; Fitzjarrald and Lenschow, 1983). It is defined by  $z/h \leq 0.1$ , where  $z$  is the height and  $h$  is the depth of the ABL (see Holtslag and Nieuwstadt, 1986, for a classification of scaling regions in clear boundary layers). These seminal articles were followed by a large number of numerical studies. These studies were concerned mainly with determining whether the descriptions used to calculate the first- and second-order moments for inert scalars, such as temperature, could also be used to calculate the same moments for chemically

reactive species. A large part of these studies addressed the  $NO - O_3 - NO_2$  chemical scheme (see Galmarini et al., 1997a, for a review). This scheme refers to the reactions:



where  $h\nu$  denotes the radiation incident on the molecule,  $\lambda$  is the ultraviolet wavelength,  $M$  is a molecule that absorbs the excess reaction energy, and  $NO, O_3, NO_2, O_2$  and  $O$  are nitric oxide, ozone, nitrogen dioxide, molecular oxygen and atomic oxygen, respectively.

The two main reasons for selecting this chemical scheme are: first, the reaction time scales included in this scheme are similar to the turbulent time scale in the ABL; second, this chemical scheme plays an important role in the evolution of ozone in the ABL, especially in the vicinity of  $NO_x (= NO + NO_2)$  sources. Note that at some distance from the sources, the catalytical role of  $NO_x$  in radical chemistry leads to photochemical  $O_3$  formation, which will be further discussed in section 4. Other chemical schemes where the turbulent transport and chemistry equations are treated simultaneously were: the production of the aerosol constituent ammonium nitrate from the reaction of nitric acid with ammonia (Brost and Delany, 1988) and the day-time ozone evolution in a biogenically influenced environment (Gao and Wesely, 1994).

An analysis of the governing equations and the numerical results presented in the cited studies show the importance to explicitly account for the chemical terms in the first- and second-moment equations. The differences with respect to the inert scalar equations can be summarized as follows:

- (1) in conditions of steady state, horizontal homogeneity and neutral stratification, the turbulent flux of the reacting chemical compounds diverges with height. Consequently, the mean concentration deviates from the logarithmic profile that is typical for inert gases. On the assumption that these conditions prevail and in the absence of sources, equation (6) reduces to the third term on the left-hand side and the chemical term  $R_i$ . Because of the latter term, the concentration flux is no longer constant with height.
- (2) whereas the relationship between the flux and the mean concentration gradient is a function of stability for a passive and a reactive scalar, the flux-gradient relationship for reacting compounds also depends on the flux Damköhler number. This dependence is due to the chemical term  $R_{w'_\alpha c'_i}$  which appears in the flux budget equation.
- (3) the inefficient mixing of species leads to the segregation of species and therefore to a reduction in the chemical activity (Donaldson and Hilst,



1972). As mentioned earlier, the influence of turbulent mixing on chemical reactions is quantified by the intensity of segregation. It should be stressed that the non-dimensional form of the chemical term (11) is also a function of the flux Damköhler number.

The above-mentioned differences are important when the time scale of chemistry is of the same order as the transport time scale, i.e. in the moderate chemistry regime. In the surface layer, one can estimate the Damköhler number after defining the following time scale for the flow  $\kappa z/u_*$ , where  $\kappa$  is the Von Karman constant ( $= 0.4$ ) and  $u_*$  is the friction velocity. To illustrate one of the differences between inert and reactive scalar descriptions, Galmarini et al. (1997a) solved the first moment equations and the second-moment equations in the vertical direction ( $x_3 = z$ ). The numerical model calculates the vertical transport of chemical species under any stability condition and for any chemical scheme. Figure 1 shows the vertical profiles of the flux-gradient relationships  $\Phi_{ci}$  in a neutrally stratified surface layer for the chemical triad  $NO - O_3 - NO_2$  (reactions 14-16). The term  $\Phi_{ci}$  is defined as the ratio of the mean concentration gradient to the vertical concentration flux. In the absence of any chemical reaction (inert scalar), this quantity is expected to be constant with height and to be equal to one ( $\Phi_h = 1$ ). The figure clearly shows a deviation from this behaviour. The Damköhler numbers for  $NO$ ,  $O_3$  and  $NO_2$

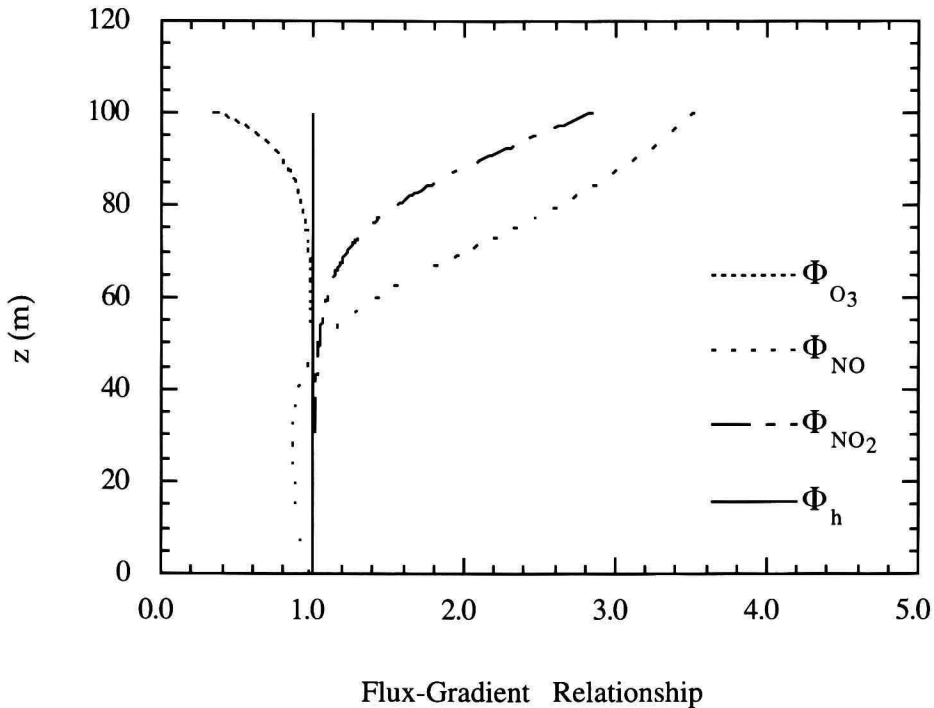


Fig. 1. Vertical profile of the flux-gradient relationship of  $NO$ ,  $NO_2$ ,  $O_3$  and temperature in a neutral surface layer.

at the top of the surface layer are 2.9, 0.05 and 0.7, respectively. These values show that the largest deviations are found for the largest Damköhler numbers. In other words, as the Damköhler number increases, the chemical term in the flux equation plays a more dominant role. However observations to confirm the behaviour seen in Figure 1 are lacking. Typically, only emission and deposition fluxes are observed at one level (Duyzer and Fowler, 1994; Foken et al., 1995).

Research has been confined mainly to numerical modelling because of the lack of high-frequency measurements (currently only a few species such as  $H_2O$ ,  $SO_2$ ,  $CO_2$ ,  $O_3$  and  $NO_2$  can be measured by means of the eddy correlation technique) as well as the relatively high instrument detection limits. Moreover, concentration profiles representative of the ABL can only be obtained by aircraft. Nevertheless, it is expected that future measurement campaigns will yield experimental verification of the three points raised above.

### 3.2 Convective boundary layer

The turbulent characteristics of the Convective Boundary Layer (CBL) play an important role in the mixing and transformation of reactive species. The vigorous and narrow updrafts may transport the emitted species from the surface to the top of the CBL. A counter-flow is then established which is characterized by weaker and larger scale downdrafts that may carry entrained species from the free troposphere to the surface. To mimic these conditions, Direct Numerical Simulations (DNS) and Large-Eddy Simulations have been performed (Schumann, 1989; Sykes et al., 1994; Beets et al., 1996; Molemaker and Vilà-Guerau de Arellano, 1998). Second-order closure models using the additional chemistry terms in the governing equations equations have also been developed to study a similar flow (Verver et al., 1997). Several aspects of the atmospheric turbulent reacting flow under various conditions are analyzed by these studies, e.g. sensitivity analyses of the Damköhler number and of the locations of the reaction zones. Attention is also given to the quantities of emissions and entrainment, and to the background concentrations. The studies all focused on a general isothermal second-order reaction, i.e.  $A + B \xrightarrow{k} Products$ .

As an example we now present the case of a species  $A$  emitted at the surface and a species  $B$  entrained at the top of the CBL (Molemaker and Vilà-Guerau de Arellano, 1998). The initial concentrations are zero and both species are introduced into the boundary layer with the same flux value, but of opposite sign; i.e. at the top and the bottom of the CBL. Two key aspects of the influence of the CBL on chemical reactions are described here: the location of the reaction zones and the magnitude of the species separation.

The results presented have been simulated by means of DNS and correspond to a Damköhler number of 1.71. The flow time scale is  $h/w_*$ , where  $h$  is the CBL height and  $w_*$  is the convective velocity. Figure 2 shows an hor-

horizontal cross section of the reaction product  $k c_a c_b$  and the vertical velocity near the surface ( $z/h = 0.1$ ). The figure shows that the reaction takes place in the core of the updraft. Near the top (not plotted) the reaction occurs in the downdraft.

The physical interpretation of these results is given below. The emitted species A is entrained at the thermal updraft by the horizontal flow. This flow contains an excess of reactant B that has been brought down by the downdraft. Both species are then advected horizontally, mixed and chemically transformed in the updraft. The reaction is completed as the air mass is transported to the top. Any remaining species A is carried to the top where a similar

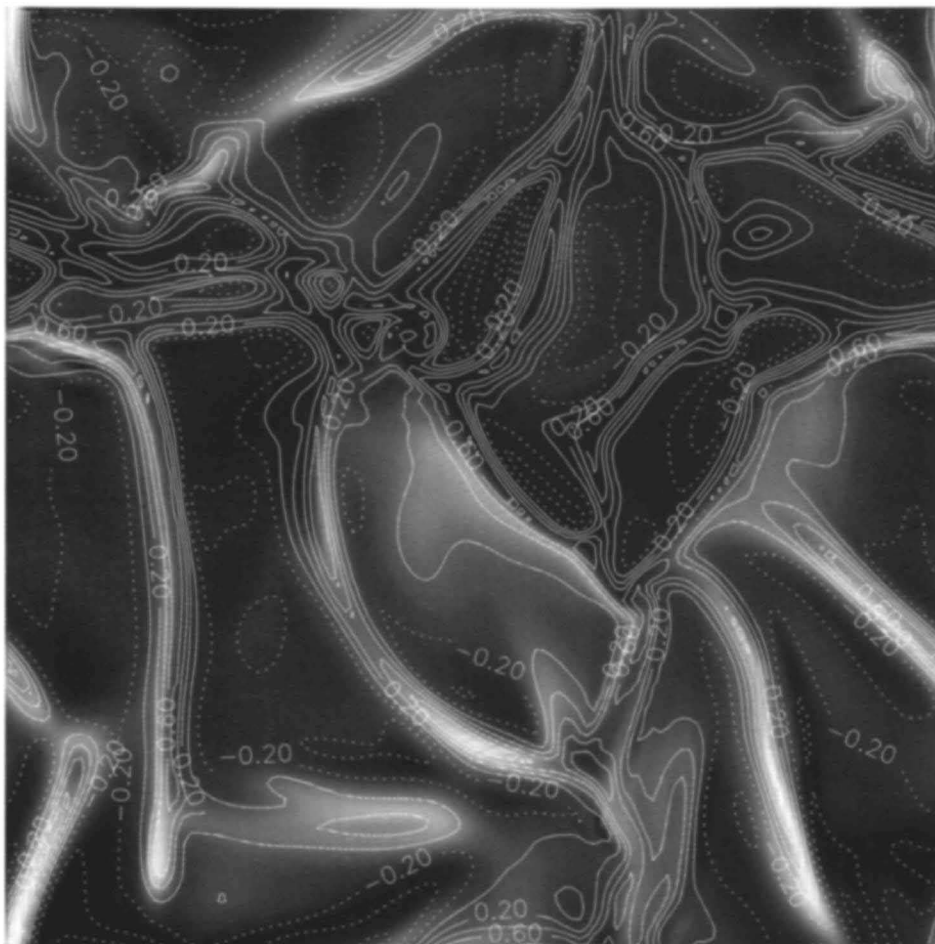


Fig. 2. Horizontal cross sections of the dimensionless vertical velocity ( $w$ ) and reaction rate ( $kC_A C_B$ ) for a turbulent reacting flow with a Damköhler number equal to 1.71 at  $z/h = 0.1$ . The reaction rate has been scaled with the maximum of the dimensionless reaction rate  $k(C_A C_B)_{max} = 1.7 \cdot 10^{-4}$ . Positive values for the vertical velocity are upward motions. The white (black) colours indicate the maximum (minimum) chemical reaction rate.

process takes place, but now in the downdraft. The simulations also show that the reaction zone location depends on the Damköhler number: the reaction zone is confined closer to the boundaries for larger values of this number.

The vertical profiles of the intensity of segregation  $I_s$  (horizontally averaged) for different Damköhler numbers corroborate this behaviour (Figure 3). All the profiles have a similar shape: smaller (negative) values of  $I_s$  at the reaction zones and larger (negative) values in the bulk of the CBL, indicating increasing segregation in this part of the CBL. These results show that the reaction rate is reduced with respect to the case where the species are homogeneously mixed due to the separation of species. It should also be mentioned that for the larger  $Da$  ( $=13.27$ ) simulation,  $I_s$  almost reaches the limiting minimum value  $-1$  in the bulk of the CBL, i.e. the reaction is confined to an infinitely thin layer. The average reaction term is enhanced when the species are introduced simultaneously at the same boundary (premixed case), resulting in positive values of  $I_s$ .

It is expected that further numerical studies of this kind will follow this line of research. Several subjects have not been studied yet. For instance, more complete and realistic chemistry should be simulated in the CBL. Another important issue concerns the chemical terms in the subgrid scale (SGS)

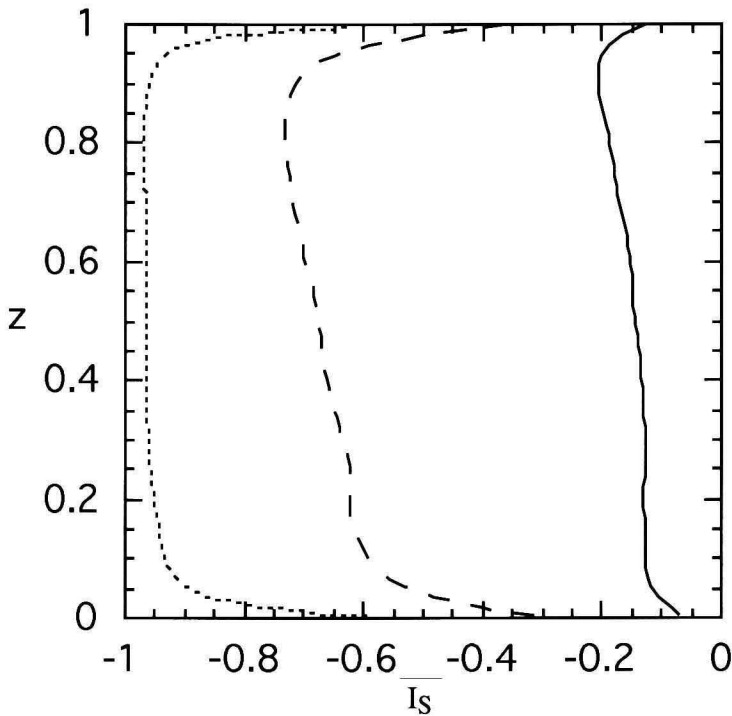


Fig. 3. Vertical profile of the intensity of segregation for the following Damköhler numbers:  $Da = 0.34$  (solid line),  $Da = 1.71$  (dashed line) and  $Da = 13.27$  (dotted line).

descriptions for the LES. Schumann (1989) omitted these chemical contributions assuming that the chemical terms of the covariance equation (11) are smaller than the transport terms. However, for fast reactions where the chemical time scale is smaller than the smallest scale of the flow, one would expect these SGS chemical terms to be of the same order of magnitude as the rest of the terms in the covariance equation and, consequently, they should be taken into account.

### 3.3 Stable boundary layer

The Stable Boundary Layer (SBL) is normally a shallow layer where buoyancy effects counterbalance vertical movements. The radiative cooling of the surface leads to a temperature gradient which generates stable stratification. This SBL structure has the following direct effects on the atmospheric chemistry:

- (1) the vertical mixing is strongly suppressed and, consequently, species are not well mixed in the vertical direction.
- (2) a large number of atmospheric chemical reaction rates depend on the temperature (see reaction term on equation 3). This dependence causes considerable space and time variations in the reactivity.

Galmarini et al. (1997b) have modelled the oxidation of nitrogen oxides through reaction with ozone in a nocturnal stable boundary layer. They developed a one-dimensional model that closes the turbulent fluxes of momentum, temperature, moisture and the five chemical species by means of a second-order closure model which includes the terms (9), (10) and (11) and assumes horizontal homogeneity and steady-state.

Figure 4 shows the vertical evolution of ozone ( $O_3$ ). From the figure one can observe two different zones with different chemistry regimes: the reservoir layer, where  $O_3$  remains almost constant, and the SBL, where the  $O_3$  concentration distribution is largely influenced by the vertical stratification. In this region,  $O_3$  is depleted by chemical transformation. One observes that the chemistry in the SBL is decoupled from the chemistry of the reservoir layer.

The separation of the species due to the stratification is quantified by the vertically averaged intensity of segregation (Figure 5). For the chemical scheme under study, the two most relevant  $I_s$  time evolutions are shown in the figure. As in the CBL, negative values are obtained for non-premixed species and, consequently, the reaction rate is reduced due to the inability of turbulence to mix the chemical reactants.

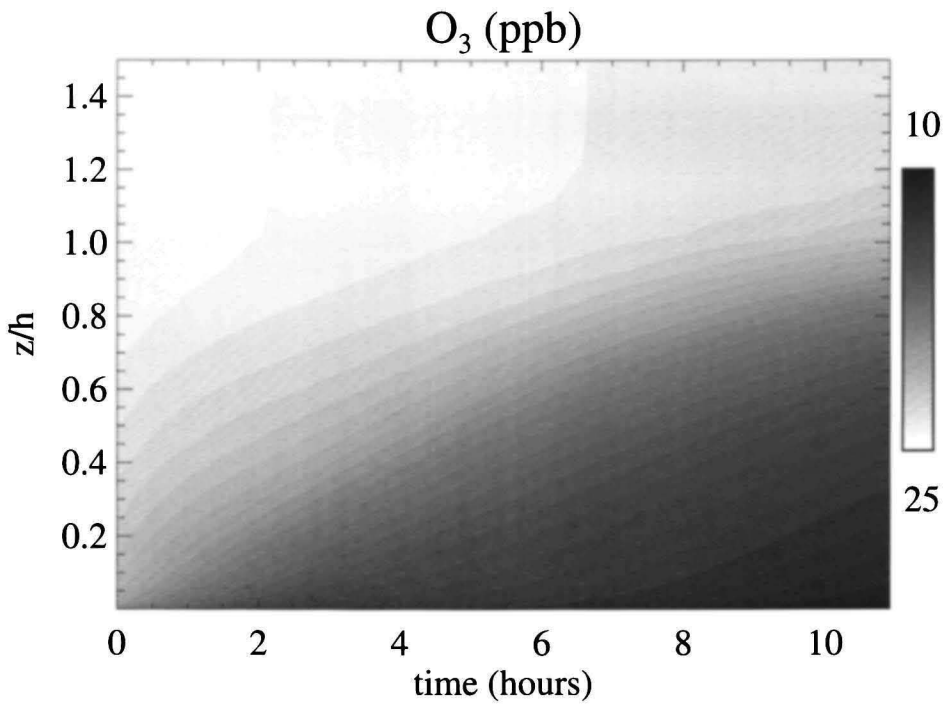


Fig. 4. Time evolution of the vertical profile of  $O_3$  (in ppb). The scale indicates the minimum and maximum concentration of the species.

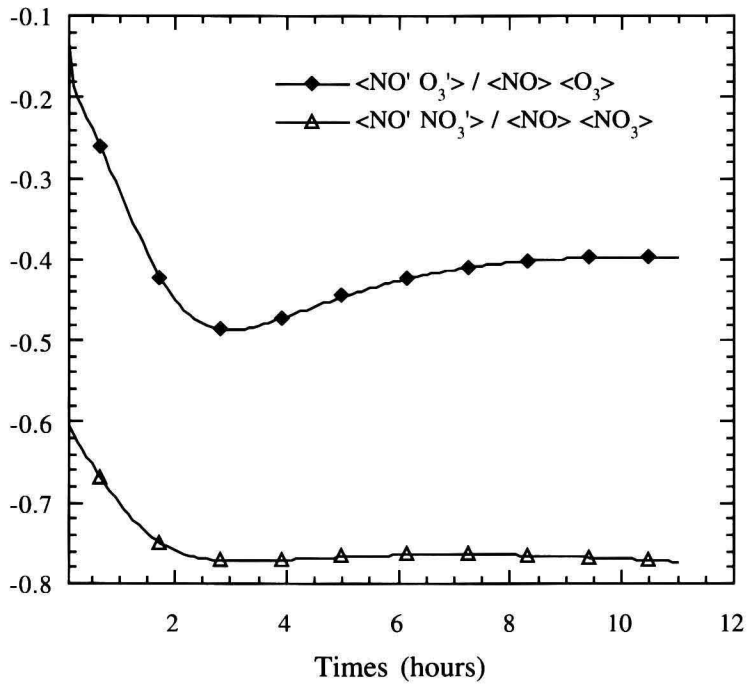


Fig. 5. Time evolution of the vertically averaged intensity of segregation.

### 3.4 Cloudy boundary layer

The presence of clouds introduces two additional effects (relative to atmospheric turbulence) which directly influence the distribution and evolution of chemical species: heterogeneous and multiphase chemistry and the effect of radiation on chemistry (see section 3.5).

Chemical reactions can occur in and at aqueous droplets and aerosol particles which are found in clouds, fogs, rain and polluted areas. These reactions are referred to as heterogeneous when they occur at surfaces (boundaries between phases) and multiphase when additional reactions occur in liquid volumes. The scavenging of species by wet deposition is also an important process that occurs in the cloudy boundary layer. The occurrence of acid deposition has given rise to numerous experimental and modelling studies concerned with the formation of sulfates, nitrates and organic acids, in particular in clouds (Seigneur, 1991).

Heterogeneous reactions can be included in models by introducing a first-order reaction rate coefficient  $k_j$  in equation (2) which accounts for the cloud or aerosol surface area  $A$  in the boundary layer. The coefficient  $k_j$  can be expressed as follows:

$$k_j = \frac{\omega_j A \gamma_j}{4}, \quad (17)$$

where  $\omega_j$  is the mean molecular speed and  $\gamma_j$  is the reactive uptake coefficient that can be experimentally determined in the laboratory (see Ravishankra, 1997, for a review). Expression (17), which represents a loss rate for reactants in the gas phase, can be extended to include aqueous phase reactions by

$$\gamma_j = \frac{4RT}{\omega_j} H_j (D_j K_j)^{1/2}, \quad (18)$$

in which  $R$  is the gas constant,  $T$  is the temperature and now  $D_j$  is the diffusion constant of dissolved gases. Assuming equilibrium of gas exchange between the droplets and their environment,  $H_j$  is the solubility constant (Henry's law).  $K_j$  denotes the first-order loss rate of dissolved gases through chemical reactions in the aqueous phase. It represents a host of reactions that can occur in solution. Some of the products of these reactions can be released to the gas phase and participate in photochemical pathways that control ozone and oxidation processes. A more complete and explicit coupling between the gas and the aqueous-phase is discussed by Lelieveld and Crutzen (1991).

Important examples of reactions that occur in clouds are sulfate formation from aqueous phase oxidation of sulfur dioxide, production of organic acids, and reduction of tropospheric ozone formation (Lelieveld and Crutzen, 1991; Lelieveld et al., 1997; Matthijsen et al., 1997). Solution chemistry in del-

iquesced sea salt particles has the potential to locally destroyed ozone (Vogt et al., 1996). In addition, it has been observed that halogen chemistry, catalyzed through heterogenous processes on ice surfaces, efficiently removes ozone to almost zero in the Artic boundary layer (Barrie et al., 1988).

Furthermore, heterogeneous removal of nitrogen oxides on pollutant aerosols and mineral dust particles can substantially affect ozone chemistry and acid production in the ABL (Dentener and Crutzen, 1993; Dentener et al., 1996). During nighttime nitrogen oxides react with ozone to form nitrate radicals and  $N_2O_5$ . The latter is rapidly converted to nitric acid on cloud and aerosols surfaces. This mechanism can substantially reduce the amount of  $NO_x$  available for photochemical ozone formation after sunrise.

### 3.5 The effect of radiation on chemistry

Important chemical species such as ozone and nitrogen dioxide are photodissociated by ultraviolet radiation in the ABL. This radiation field is strongly modified due to the presence of cloud droplets and aerosols. The net effect of multiple scattering, i.e. increase of the effective photon path length, can substantially enhance in-cloud photochemistry compared to the clear sky (Madronich, 1987; Lelieveld and Crutzen, 1991). Consequently, the first-order reaction rates or photodissociation coefficients which depend on the actinic flux are altered under cloudy conditions.

The photodissociation rate is normally expressed by the symbol  $J_j$ , which is equivalent to  $k_j$  in equation (2), and is calculated by

$$J_j = \int_{\Delta\lambda} \sigma_j(\lambda) \varphi_j(\lambda) , F(\lambda) d\lambda \quad (19)$$

where  $\sigma_j(\lambda)$  and  $\varphi_j(\lambda)$  are the wavelength ( $\lambda$ ) dependent absorption cross section and quantum yield, respectively. These functions are molecular properties determined in the laboratory.  $F(\lambda)$  is the omnidirectional actinic flux that can be understood as the photon density times the velocity of light ("actinic" pertains to radiation that can initiate photodissociation). It is calculated through

$$F(\lambda) = \int_{-\pi}^{\pi} \int_{-\pi/2}^{\pi/2} L(\theta, \phi) \sin\theta d\theta d\phi . \quad (20)$$

$L(\theta, \phi)$  is the radiance which is a function of the radiant energy.  $\theta$  and  $\phi$  are spherical coordinates, the former the angle of the beam to the surface normal. For undiffused light this is the zenith angle.

Madronich (1987) and Van Weele and Duynkerke (1993) calculated the



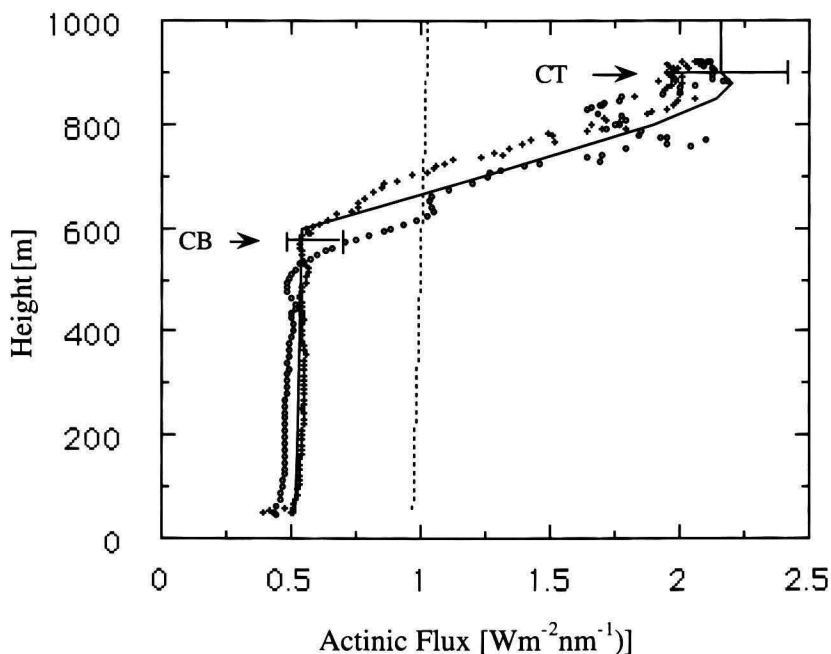


Fig. 6. Vertical profile measurements (0.1 Hz) and model calculations (solar zenith angle 38, cloud optical depth 23) of the actinic flux made on June 13, 1992. Crosses represent upsounding, open circles represent downsounding. The solid line is the vertical profile calculated with the model in the presence of a cloud. The dotted line is the vertical profile calculated with the model for the same case, but clear sky situation. Error bars represent the model variability due to the change in the solar zenith angle and cloud optical depth during the sounding. CB is cloud base; CT is cloud top.

vertical profiles of actinic fluxes for a homogeneous cloud deck by means of radiative transfer models. Model results were evaluated using actinic flux measurements collected during the Atlantic Stratocumulus Transition EXperiment campaign (Vilà-Guerau de Arellano et al., 1994). Figure 6 shows one of these measured and modelled vertical profiles. A comparison with clear sky values reveals that larger values of the actinic flux are found at cloud top and smaller values are found at cloud base. Therefore reactants at the cloud top are photodissociated faster than those at cloud base.

#### 4 Large-scale implications

In the previous section, it has been argued that the structure, characteristics and processes in the ABL play an important role in atmospheric chemistry. Large-scale atmospheric chemistry models need to include representations in

the form of parameterizations to introduce these interactions between physical and chemical processes (Peters et al., 1995; Dennis et al., 1996). Some of these attempts are briefly summarized here.

The previously cited studies suggest improvements in the parameterizations of the dry deposition/surface exchange process in the surface layer. These new descriptions included corrections to account for the chemical terms (Galmarini et al., 1997a). The parameterizations are particularly important for species that react in the moderate chemistry regime and that have low concentrations compared to other dominant species; for instance,  $NO$ ,  $NO_2$ ,  $NO_3$  and  $N_2O_5$  with respect to  $O_3$  (Gao and Wesely, 1994; Ganzeveld and Lelieveld, 1995).

For the CBL, Chatfield and Brost (1987) and Petersen et al. (1998) suggested a mass-flux model to represent the transport of chemically reactive species. This description accounts for the separation of species. A simpler approach can be based on the definition of effective chemical reaction rates that include the intensity of segregation (Molemaker and Vilà-Guerau de Arellano, 1998). Attempts to classify chemical reaction schemes according to the Damköhler number can be useful to determine which chemical reactions are limited by turbulence (Stockwell, 1995).

A parameterization that includes the effects of clouds on photodissociation rates in atmospheric chemistry models has been developed by Krol and Van Weele (1997). That study shows that species which react rapidly, such as  $OH$  and  $HO_2$ ; can be strongly influenced by the presence of clouds.

Parameterizations of global tropospheric chemistry processes in a general circulation model (GCM) have been developed (Roelofs and Lelieveld, 1995; Roelofs and Lelieveld, 1997). This involves descriptions of natural and pollutant gas emissions, photochemical reactions in the gas-phase, effect of clouds on photolyses frequencies, reactions on particle/droplet surfaces and aqueous phase transformations, as well as removal of reaction products by dry and wet deposition processes. Dry deposition has been modelled consistently with the GCM boundary and surface characteristics. Results from these model studies show that the removal of sulfur dioxide from the atmosphere is to a large extent determined by the dry deposition process. For instance, in the Northern Hemisphere, where most anthropogenic sulfur emissions occur, about one quarter of the  $SO_2$  emissions is removed by the dry deposition process, whereas the reaction product sulfate is largely removed through precipitation (Lelieveld et al., 1997).

ABL processes also play an important role in the control of tropospheric ozone. Chemistry-GCM simulations indicate that, on a global scale, about 60% of the tropospheric ozone is determined by photochemical formation in the troposphere while 40% originates from the stratosphere (Roelofs and Lelieveld, 1997). Ozone from the stratosphere is transported across the extratropical tropopause by the wave driven meridional circulation (Holton et al., 1995). In the Northern Hemisphere, where large scale ozone chemistry is strongly perturbed by anthropogenic emissions, much of the ozone formed in the tropo-

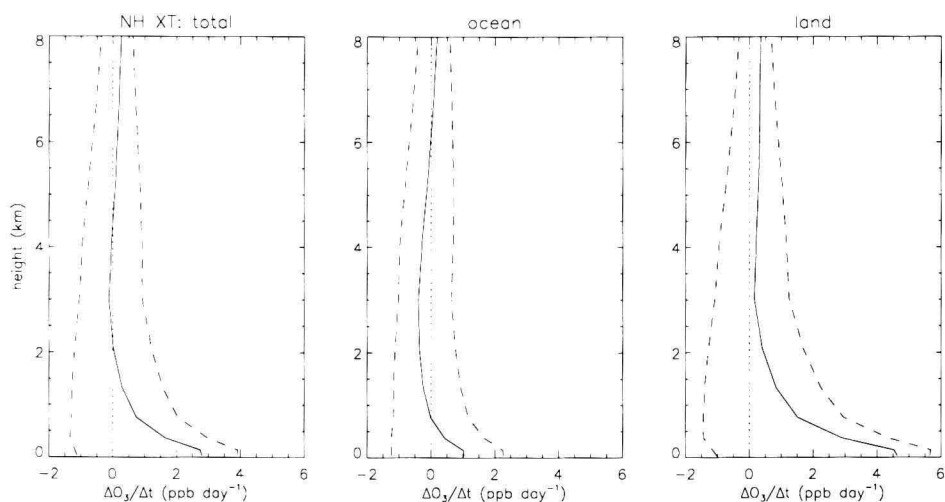


Fig. 7. Annual mean ozone production and destruction rates (dashed lines) in the lower atmosphere in the Northern Hemisphere (north of  $30^\circ$  N) simulated by a chemistry-general circulation model. The solid line indicates the net ozone production, showing that in the entire Northern Hemisphere extratropics ozone formation prevails in the lower 2 km of the atmosphere.

sphere results from chemical processes in the ABL, both in the tropics and in midlatitudes. Typically, pollutant  $O_3$  is formed over land and destroyed during transport over the oceans. However, in the North Atlantic region, where polluted air is transported from the USA to Europe, ozone formation in the boundary layer can still be significant. In fact, pollutant emissions in the extratropical Northern Hemisphere cause large-scale ozone production, both in the continental and marine boundary layer (Figure 7). On the other hand, in the Southern Hemisphere, especially over the remote oceans, net ozone destruction dominates.

## 5 Conclusions

Atmospheric boundary layer characteristics and processes can largely influence chemical reactions. Evidently, it remains a challenge to represent the main complex interactions between physical and chemical processes in the ABL for large scale atmospheric chemistry models. Most of these models still neglect the rate limiting influence of turbulent mixing on important photochemical reactions that occur on timescales of minutes or even less. These processes can be accounted for by deriving relatively simple "correction" factors that can be applied to the reaction rate coefficient  $k_j$ , i.e. effective reaction rates.

Since the surface and volume of aerosols and liquid water droplets is considerable in the ABL, heterogeneous and multiphase reactions should be

accounted for as well. Further studies should be performed to obtain experimental evidence of the influence of ABL processes in atmospheric chemistry. Measurements campaigns have to be specifically designed to gain a better understanding of the mentioned effects and to validate current numerical models.

The implementation of more complex chemical mechanisms in LES is also an issue of future research. This extension will bring the possibility to study the spatial distribution and time evolution of species that react under different time scales with respect the flow time scale. Another important aspect to study, will be the role of chemical equilibria in turbulent reacting flows. Additional aspects that need further explorations include interactions between vegetated surfaces and the atmosphere, for example, in representing natural emissions and dry deposition of chemical species and aerosols. It may be expected that the greater amount of detail and resolution of regional and global models, associated in part to greater computer power, will provide opportunities to develop and implement parameterizations of the above mentioned processes.

### **Acknowledgement**

We are grateful to S. Galmarini, M. Krol, J. Matthijssen, J. Molemaker, G.J. Roelofs and G. Verver for valuable comments and suggestions during the preparation of this chapter. One of the authors (J. Vilá) is partially supported by a NATO research grant (CRC 970040).